NUCL SCI TECH (2018) 29:168
https://doi.org/10.1007/s41365-018-0494-x

A 4H–SiC betavoltaic battery based on a ^{63}Ni source

Yu-Min Liu[1] · Jing-Bin Lu[1] · Xiao-Yi Li[1] · Xu Xu[1] · Rui He[1] · Hui-Dong Wang[1]

Received: 10 December 2017 / Revised: 23 March 2018 / Accepted: 10 April 2018 / Published online: 13 October 2018

Abstract A 4H–SiC–^{63}Ni p–n-junction-based betavoltaic battery is investigated. The Monte Carlo method is used to simulate the self-absorption effect of the^{63}Ni source, the backscattering process, and the transport of beta particles in 4H–SiC material. The main factors that affect the energy conversion efficiencies of the cell are analyzed. Based on the simulation results, it can be calculated that, when the thickness of the ^{63}Ni source increases from 2×10^{-3} to 10 μm, the theoretical maximum device conversion efficiency increases from 16.77 to 23.51% and the total conversion efficiency decreases from 16.73 to 1.48%. Furthermore, a feasible design with a maximum output power density of 0.36 μW/cm^2 and an optimal device conversion efficiency of 23.5% is obtained.

Keywords 4H–SiC–^{63}Ni betavoltaic battery · p–n junction · Energy conversion efficiency

1 Introduction

Nuclear batteries have attracted the interest of researchers as far back as the 1900s [1]. In recent decades, betavoltaic batteries have been intensively demonstrated. The structure mainly contains a beta source and an energy converter such as a p–n junction, a p–i–n junction, or a Schottky barrier diode [1–21]. In these energy converters, beta particles interact with matter and the ionizing radiation generates electron–hole pairs. The electron–hole pairs, which are generated in or near the depletion region, can be separated and eventually swept out of this region by the built-in potential barrier. Then they are collected for the radiation-induced current formation, thereby converting the decay energy into electrical energy directly [1, 10, 13]. The performance of a betavoltaic cell is determined by the radioisotope, radiation transport properties of beta particles in matter, and the energy converter. Compared with micro-chemical cells and micro-solar cells, the advantages of betavoltaic batteries mainly include easy integration on a small scale, stable performance, long service lifetime, high energy density, self-sustainability, and little maintenance [2–20]. Therefore, such batteries have become a promising micro-power source for micro-electronic mechanical systems (MEMSs), medical applications such as pacemaker power, and applications in execrable ambient such as space exploration [2–20].

Previous research has shown that SiC material and a ^{63}Ni source are suitable for p–n-junction-based betavoltaic batteries. For example, in 2006, a micro-battery with a 1 mCi ^{63}Ni source on an n$^+$p SiC structure was reported. An open-circuit voltage of 0.72 V and a short-circuit current density of 16.8 nA/cm^2 were measured [3]. In 2015, the Monte Carlo method was used to investigate a 4H–SiC cell with a ^{63}Ni source. The maximum device conversion efficiency was 25.04% when the thickness of the source was 6 μm [9]. In 2016, another 4H–SiC–^{63}Ni cell was studied by using the Monte Carlo method and a Synopsys Medici device simulator. The simulation results showed that the

This work was supported by the National Major Scientific Instruments and Equipment Development Project (No. 2012YQ240121) and the National Natural Science Foundation of China (No. 11075064).

✉ Jing-Bin Lu
ljb@jlu.edu.cn

[1] College of Physics, Jilin University, Changchun 130012, China

total conversion efficiency decreased from 13.65 to 1.52% when the thickness of the source increased from 0.1 to 5 μm [10].

In this research, we analyze the main factors that affect the energy conversion efficiencies of 4H–SiC–^{63}Ni p–n-junction-based batteries. Based on the simulation results, theoretical maximum electrical properties and energy conversion efficiencies are calculated. Finally, the light p-type region is selected as the emitter layer and the high n-type region is used as the base layer. Then the p–n junction is designed to match the depletion region with the main energy deposition region of the ^{63}Ni source in 4H–SiC material. An optimal design that has a maximum output power of 0.36 $\mu W/cm^2$ and a device conversion efficiency of 23.5% is then proposed. These results are helpful for designing practical cells. Although 4H–SiC material and a ^{63}Ni source are used in this study, the simulated and calculated model can be extended to explore other semiconductor materials and beta sources for betavoltaic batteries.

2 Selection of materials and sources

4H–SiC is a wide-band-gap semiconductor material. The band gap and the intrinsic carrier concentration are $\sim$3.25 eV and $\sim 9.5 \times 10^{-9}$ cm^3 at 300 K, respectively [1]. The wide band gap and the low intrinsic carrier concentration contribute to the high energy conversion efficiency and high radiation resistance of nuclear batteries [1, 10]. In the interaction of beta particles with the target material, electron–hole pairs are generated as well as heat. The fraction of energy that goes into electron–hole pair formation is calculated as the band gap energy E_g divided by the mean ionization energy E_{ehp}. This ratio represents the ultimate conversion efficiency η_{ult} of the electron-hole pairs production efficiency [1]. The mean ionization energy is confirmed as $E_{ehp} = 2.8E_g + 0.5$ in Ref. [9]. As shown in Fig. 1, the ultimate conversion efficiency increases and then nearly reaches its saturation value with increasing band gap. For 4H–SiC material, the ultimate conversion efficiency is 33.8%. Thus, 4H–SiC material is fit for betavoltaic cells.

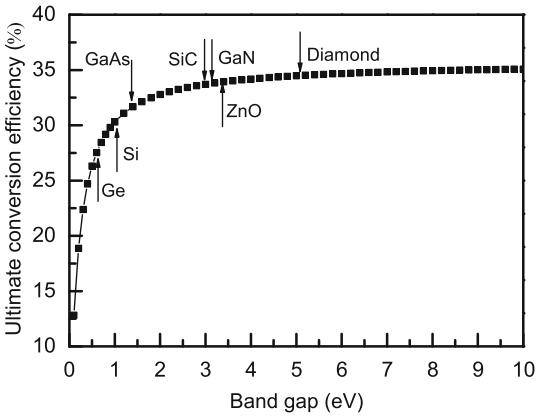

Fig. 1 Ultimate conversion efficiency versus band gap

The sources for betavoltaic batteries are listed in Table 1 [1, 2, 8]. In general, high incident energy results in high electrical power in a certain volume. The average decay energy E_{ave} of a ^{3}H source is low for high-energy devices. A ^{35}S source is not suitable for long-term applications owing to its short half-life $T_{1/2}$. A ^{63}Ni source is the main candidate for betavoltaic cells because of its pure beta radiation, long half-life, and the moderate average decay energy. Moreover, the maximum decay energy β_{max} of a ^{63}Ni source is below the threshold energy of radiation damage in most semiconductor materials [4, 5, 8]. For a ^{85}Kr source and a ^{147}Pm source, their maximum decay energies are high and they are both gamma emitters (^{85}Kr : 0.4% for γ emission and ^{147}Pm : 0.003% for γ emission) [1, 8]. The high-energy beta particles and the gamma rays may badly damage the lattice structure of semiconductor materials. A ^{90}Y source is also a beta emitter and it is produced from the decay of a ^{90}Sr source. Therefore, a ^{90}Sr source is a mixture of ^{90}Sr and ^{90}Y sources, and the average decay energy is 1.1 MeV [8]. This decay energy is excessively high for 4H–SiC material. Therefore, a pure ^{63}Ni source is suitable for 4H–SiC betavoltaic batteries. In addition, a ^{63}Ni source is easier to handle because of its solid-metal form.

3 Simulation results and discussion

The Monte Carlo method is used to simulate the self-absorption effect of the ^{63}Ni source, the backscattering process, and the transport of beta particles in 4H–SiC material. Then we analyze the main factors that affect the energy conversion efficiencies of 4H–SiC–^{63}Ni cells.

3.1 Self-absorption effect of source

Beta particles dissipate their energy within the source itself and this phenomenon is referred as self-absorption.

Table 1 Sources for betavoltaic batteries

Isotope	^{3}H	^{35}S	^{63}Ni	^{85}Kr	^{90}Sr	^{90}Y	^{147}Pm
$T_{1/2}$ (years)	12.3	0.24	100.2	10.7	28.8	0.007	2.6
β_{max} (keV)	18.6	168	66.7	670	546	2280	225
E_{ave} (keV)	5.7	48.8	17.4	251	195.8	945	62

The self-absorption loss η_{sel} is defined as the energy deposited in the source divided by the total energy produced in the source. In the simulated model, the energy spectrum of the ^{63}Ni isotope is shown in Fig. 2 [19]. Its geometrical structure is cuboid and its cross-sectional area is 1×1 cm^2.

In Fig. 3, it can be seen that, when the thickness of the ^{63}Ni layer increases from 2×10^{-3} to 10 μm, the apparent power density increases from 1×10^{-2} to 3.24 μW/cm^2 and the self-absorption loss increases from 0.036 to 93.7%. Moreover, when the thickness of the source is 2 μm, the apparent power density is 3.1 μW/cm^2 and the self-absorption loss is 70%. For 0.004-, 0.1-, 0.3-, 1-, 1.6-, 2-, 4-, 6-, and 10-μm-thick ^{63}Ni sources, the emitted energy spectra are shown in Fig. 4. It can be seen that the peaks of these emitted energy spectra move toward the higher energy region and then mostly keep fixed as the thickness of the source increases. Finally, as shown in Fig. 5, when the thickness of the ^{63}Ni layer increases from 2×10^{-3} to 10 μm, the average energy of the emitted energy spectrum increases from 17.5 keV to a maximum value of 21.24 keV at ~2 μm. These results can be explained as follows: When the source is thin, low-energy beta particles are easily absorbed while high-energy beta particles have a chance to escape from the source. However, if the source is thick enough, even high-energy beta particles in deep positions can barely emit from the beta source.

3.2 Directional loss

The typical prototype of a p–n-junction-based betavoltaic cell is illustrated in Fig. 6 [6, 12, 14]. In such a structure, less than half of the emitted beta particles can reach the surface of the energy converter. Then the directional loss η_{dir} is defined as the number of beta particles that do not reach the surface of the energy converter divided by the total number of beta particles emitted from the source [9]. In a practical cell, the same energy converter is usually set on the other side of the source. Therefore, a stacked structure is the main method used to decrease directional loss [7].

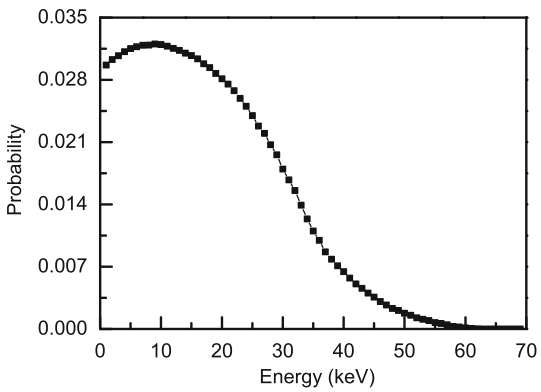

Fig. 2 Energy spectrum of the ^{63}Ni isotope

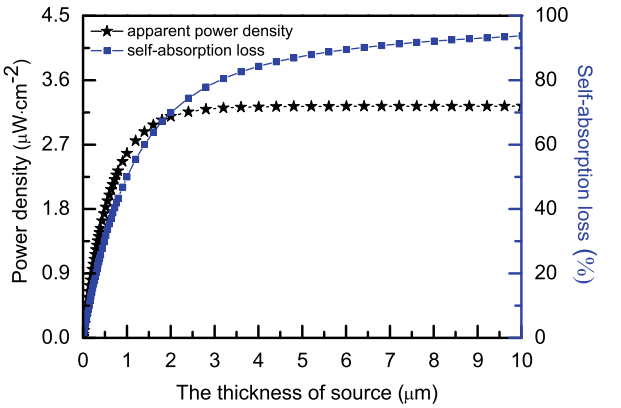

Fig. 3 Apparent power density and self-absorption loss versus the thickness of the ^{63}Ni source

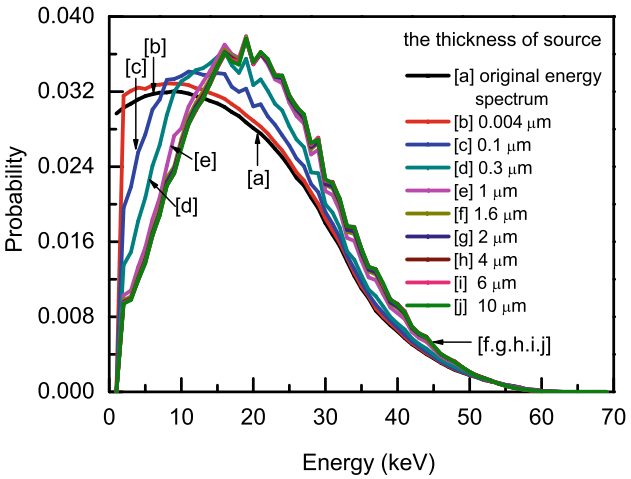

Fig. 4 Emitted energy spectra of the ^{63}Ni source with different thicknesses

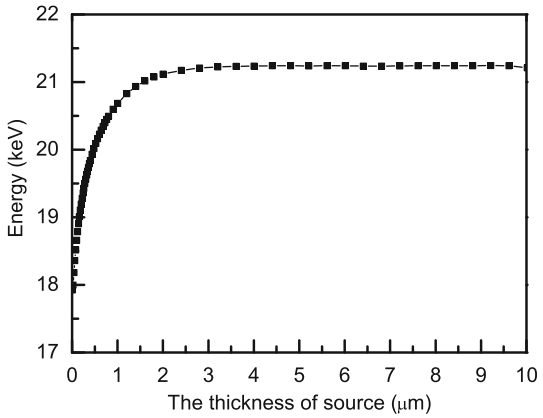

Fig. 5 Average energy of the emitted energy spectrum versus the thickness of the ^{63}Ni source

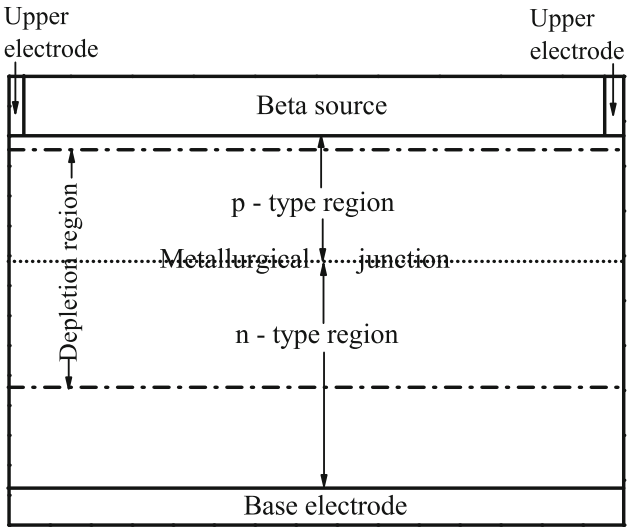

Fig. 6 Prototype of the p–n-junction-based betavoltaic cell

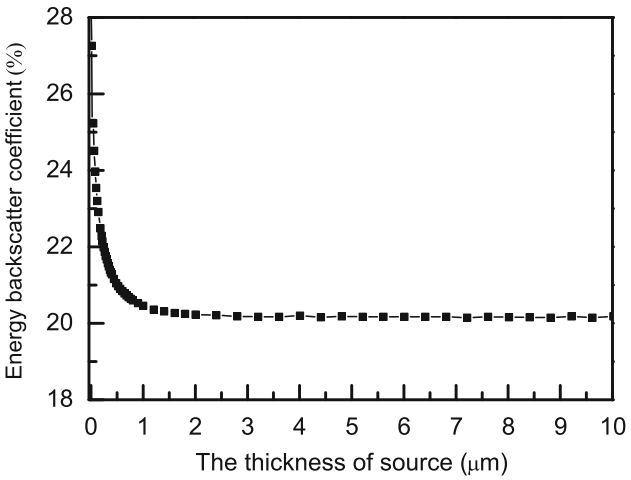

Fig. 7 Energy backscatter coefficient on the surface of 4H–SiC material versus the thickness of the ^{63}Ni source

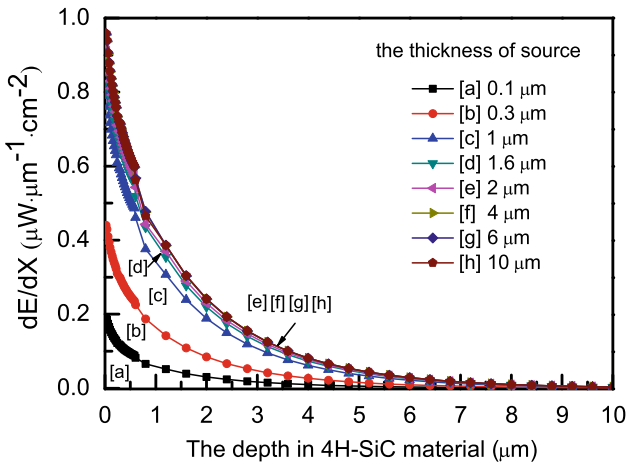

Fig. 8 (Color online) Power density deposition per unit length versus the depth in 4H–SiC material

3.3 External interaction loss

The external interaction loss is described as the energy loss between the source and the energy converter [9]. One part of the external interaction loss is the energy deposited in the dead layer, which mainly contains the metal electrode layer, the narrow air layer, and the passivation layer on the surface of cell. Generally, the scale of the dead layer is tens of nanometers and the energy deposited in this region can be neglected [1]. Another part of the external interaction loss is the energy backscattering loss on the surface, which is a significant energy loss in betavoltaic cells. The energy backscattering coefficient η_{sca} is defined as the reflected energy divided by the total energy entering the energy converter. A theoretical analysis shows that the low atomic number of 4H–SiC material and the high energy of the ^{63}Ni source contribute to the small energy backscattering coefficient. In this study, the energy converter consists only of 4H–SiC material. Its geometrical structure is cuboid and the junction area is 1×1 cm^2. Moreover, the beta source is placed close to the surface of the energy converter and the whole device is set in vacuum. In Fig. 7, it can be seen that, when the thickness of the ^{63}Ni layer increases from 2×10^{-3} to 10 μm, the energy backscattering coefficient on the surface of the 4H–SiC material device decreases from 28.77% to its minimum value of 20.15% at $\sim$2 μm.

3.4 Energy distribution and internal interaction loss

The energy distribution of beta sources in matter can be obtained by using the Monte Carlo method. Here, for 0.1-, 0.3-, 1-, 1.6-, 2-, 4-, 6-, and 10-μm-thick ^{63}Ni sources, the calculated results in Fig. 8 show that the power density deposition per unit length nearly exponentially decreases with the penetration depth increasing in 4H–SiC material. The results indicate that the maximum energy deposition per unit length takes place at the surface and that the energy of the beta source is quickly absorbed in matter. Further calculation shows that the width of the main energy deposition region, which absorbs $>$ 99% of the total energy deposited in 4H–SiC material, approaches 8 μm and is nearly identical for ^{63}Ni layers of different thicknesses. This can be explained by the fact that the emitted energy spectra are similar for various source thicknesses. Therefore, a thin 4H–SiC membrane close to the source is needed to absorb the energy of the ^{63}Ni source. Based on the beta source energy distribution law in matter, it is concluded that the p–n junction, the p–i–n junction, and the Schottky barrier diode are appropriate for betavoltaic cells, because an internal electrical field exists and their depletion

regions can be designed to match the main region of ionizing radiation. Furthermore, the simulation results show that the maximum penetration depth of the ^{63}Ni source in 4H–SiC material is nearly 23 μm and is independent of the source thickness, because the maximum penetration depth of beta particles in matter is determined by the maximum decay energy of the beta source.

In the p–n-junction-based cell, the electron–hole pairs generated in the depletion region are eventually separated and then collected for the radiation-induced current formation. The charge collection efficiency (CCE) in the depletion region is 100% [1]. However, the electron–hole pairs generated outside the depletion region, which must diffuse into the depletion region, can be separated and collected. Therefore, the depletion region and its nearby region, which is about one diffusion length of minority carrier away from the edge of depletion region, are referred to as the active region in a cell. The charge collection efficiency outside the active region can be neglected [1, 12, 15]. The energy transport efficiency η_{dpl} can then be defined as the energy deposited in the active region (P_{dep}) divided by the apparent energy of the source (P_{sur}) entering the energy converter. Moreover, the energy deposition outside the active region is described as the internal interaction loss in the cell.

The total energy deposited in the energy converter represents the maximum available energy for electron–hole pairs generation. Based on the simulation results, when the thickness of the ^{63}Ni layer increases from 2×10^{-3} to 10 μm, the total energy deposited in 4H–SiC material increases from 3.71×10^{-3} to 1.53 μW/cm^2. Moreover, when the thickness of the source is 2 μm, the total power density deposited in 4H–SiC material is 1.46 μW/cm^2. These results are shown in Fig. 9.

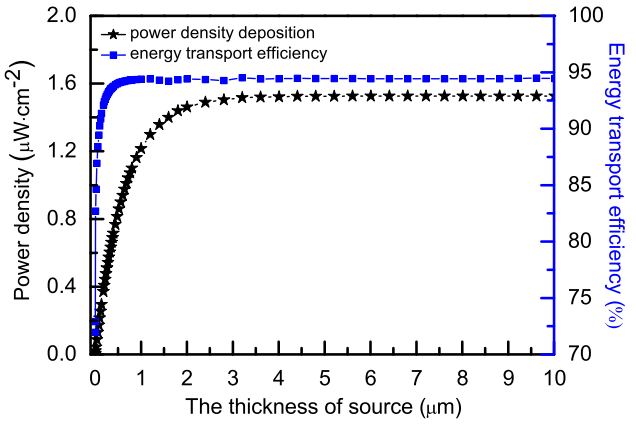

Fig. 9 (Color online) Total power density deposited in 4H–SiC material and the energy transport efficiency versus the thickness of the ^{63}Ni source

Further analysis shows that the energy deposited in 4H–SiC material is greater than the difference between the incident energy and the backscattering energy on the surface. This result may be attributed to multiple backscattering of beta particles on the source and device surfaces. Finally, if the energy deposited in 4H–SiC material is totally in the active region of the cell, the energy transport efficiency increases from 72 to 94% and it nearly reaches a saturation value at 1 μm when the thickness of the ^{63}Ni layer increases from 2×10^{-3} to 10 μm. The result is plotted in Fig. 9.

4 Optimal cell design

4.1 Theoretical electrical properties

In a betavoltaic cell, the short-circuit current density J_{sc} is given by [1]

$$J_{\mathrm{sc}} = \frac{\mathrm{CCE} \cdot q \cdot P_{\mathrm{dep}}}{S \cdot E_{\mathrm{ehp}}}, \tag{1}$$

where CCE is the electron–hole pair collection efficiency, q is the unit electron charge, P_{dep} is the energy deposited in the active region, S is the junction area, and E_{ehp} is the mean ionization energy. The open-circuit voltage V_{oc} is given by [9]

$$V_{\mathrm{oc}} = \frac{k_{\mathrm{B}}T}{q} \ln\left(\frac{J_{\mathrm{sc}}}{J_0} + 1\right), \tag{2}$$

where k_{B} is Boltzmann's constant, T is the absolute temperature, and J_0 is the minimum ideal reverse saturation current density, which is confirmed as $J_0 = 1.5 \times 10^5 \exp(-E_{\mathrm{g}}/k_{\mathrm{B}}T)$ in A/cm^2 in Ref. [9]. During the calculations, we assume that the total energy deposited in 4H–SiC material is in the active region and that the charge collection efficiency is 100%. As shown in Fig. 10, when

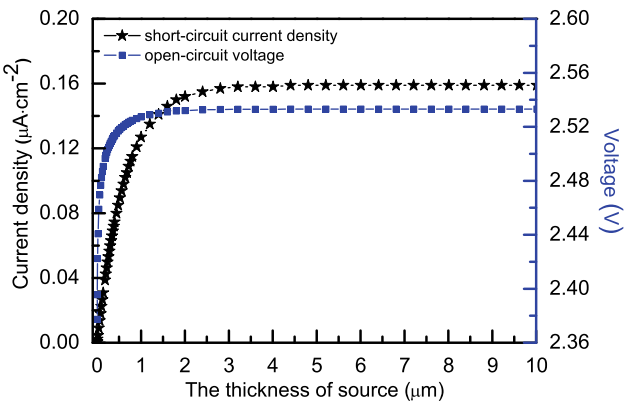

Fig. 10 (Color online) Ultimate short-circuit current density and open-circuit voltage versus the thickness of the ^{63}Ni source

the thickness of the ^{63}Ni layer increases from 2×10^{-3} to 10 μm, the short-circuit current density increases from 3.87×10^{-4} to 0.16 μA/cm^2 and the open-circuit voltage increases from 2.38 to 2.53 V at 300 K.

In Fig. 10, compared with the short-circuit current density, it can be seen that the open-circuit voltage is insensitive to the thickness of the ^{63}Ni layer. The main reason for this is that the minimum ideal reverse saturation current is much smaller than the short-circuit current. Experimental tests have shown that the open-circuit voltage is mainly affected by the reverse saturation current [8]. In a p–n-junction-based energy converter, the reverse saturation current is mainly determined by the physical parameters of the material and the semiconductor manufacturing technology [1]. Moreover, the more radiation damage that exists, the greater the number of internal defects is created and then the reverse saturation current increases. Finally, the ratio, which is the open-circuit voltage to the band gap, is defined as the driving potential efficiency η_p of the cell [1]. The calculated result shows that, when the thickness of the ^{63}Ni layer increases from 2×10^{-3} to 10 μm, the theoretical maximum driving potential efficiency increases from 73.2 to 77.8% and it nearly reaches its maximum value at 2 μm in the 4H–SiC–^{63}Ni cells.

The net current density J of the cell, which is in the reverse-biased direction, is given by [22]

$$J = J_{sc} - J_0\left[\exp\left(\frac{qV}{k_B T}\right) - 1\right], \tag{3}$$

where V is the voltage across the resistive load. For 0.1-, 0.3-, 1-, 1.6-, 2-, 4-, 6-, and 10-μm-thick ^{63}Ni sources, the current density–voltage characteristics of 4H–SiC cells are shown in Fig. 11. The power density P delivered to the resistive load is given by

$$P = J \cdot V = J_{sc} \cdot V - J_0\left[\exp\left(\frac{qV}{k_B T}\right) - 1\right] \cdot V. \tag{4}$$

Based on Eq. (4), the maximum output power P_{max} of the cell is given by [22]

$$\left(1 + \frac{qV_m}{k_B T}\right)\exp\left(\frac{qV_m}{k_B T}\right) = 1 + \frac{J_{sc}}{J_0}, \tag{5}$$

where V_m is the voltage across the resistive load when $P = P_{max}$. Then the fill factor FF is given by

$$FF = \frac{P_{max}}{V_{oc} \cdot I_{sc}}. \tag{6}$$

As can be seen in Fig. 12, when the thickness of the ^{63}Ni layer increases from 2×10^{-3} to 10 μm, the theoretical upper limit of the maximum output power density increases from 8.7×10^{-4} to 0.38 μW/cm^2 and the fill factor increases from 94.04 to 94.32%. Moreover, the maximum output power density nearly reaches its saturation value when the thickness of the source is 2 μm and the fill factor nearly reaches its maximum value at 1 μm.

4.2 Theoretical energy conversion efficiencies

There are usually two types of energy conversion efficiencies in betavoltaic batteries. One is the device conversion efficiency η_{dev}, which is calculated by using [1]

$$\eta_{dev} = \frac{P_{max}}{P_{sur}} = \eta_{dpl} \cdot \eta_{ult} \cdot \eta_p \cdot FF, \tag{7}$$

where η_{dpl} is the energy transport efficiency of the source, η_{ult} is the ultimate conversion efficiency of the electron-hole pairs production efficiency, η_p is the driving potential efficiency of the cell, and FF is the fill factor. Another type is the total conversion efficiency η_{total}, which can be separated into the utilization efficiency of the source and the device conversion efficiency of the cell. The utilization

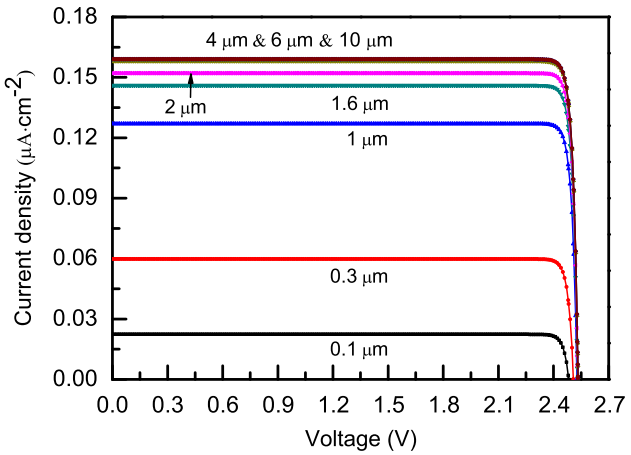

Fig. 11 (Color online) Current density–voltage characteristics of the 4H–SiC–^{63}Ni cells

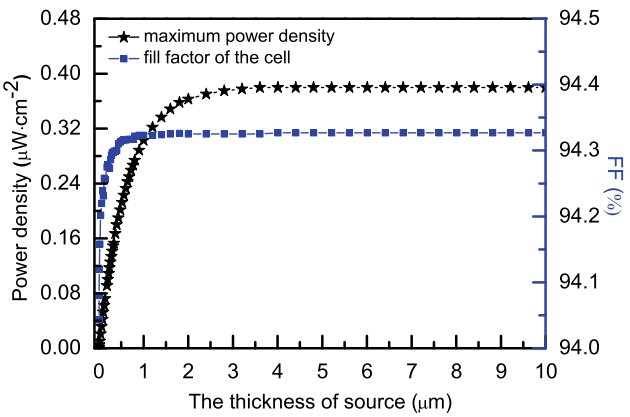

Fig. 12 (Color online) Maximum power density and FF of the cells versus the thickness of the ^{63}Ni source

efficiency of the source is mainly determined by the self-absorption loss itself and the directional loss of the cell. To minimize the directional loss, the same energy converters are usually placed on both the upper and base sides of the source in a practical cell. Therefore, the total conversion efficiency in this study is calculated by using the maximum output power of one energy converter divided by half the total power produced in the source [1, 8]:

$$\eta_{\text{total}} = \frac{P_{\max}}{P_{\text{total}}} = (1 - \eta_{\text{sel}}) \cdot \eta_{\text{dev}}, \tag{8}$$

where η_{sel} is the self-absorption loss of the source.

Now, the energy conversion efficiencies of 4H–SiC–^{63}Ni batteries can be calculated. It is shown that, when the thickness of the ^{63}Ni layer increases from 2×10^{-3} to 10 μm, the theoretical maximum device conversion efficiency increases from 16.77% to the saturation value of 23.51% at ~2μm and the total conversion efficiency decreases from 16.73 to 1.48%. The results are plotted in Fig. 13. The theoretical energy conversion efficiencies in Fig. 13 are nearly in accordance with the results reported in Refs. [9, 10]. Although the energy conversion efficiencies measured in the fabricated cells are much lower than the theoretical calculated values [2, 8, 13, 16], the results achieved in this study are helpful for optimizing the design of 4H–SiC–^{63}Ni cells. Moreover, the semiconductor manufacturing technology and the isotope loading technique need further development. Meanwhile, radiation management is also an important issue.

4.3 An optimal design of doping concentrations

In p–n-junction-based batteries, the p-type region is set as the base layer in solar cells. However, the p-type region is selected as the emitter layer and the n-type region is used as the base layer in betavoltaic cells. There are two reasons for this. The first reason is that the main energy deposition region of a beta source in matter is close to the surface of the emitter layer and it is different from that of the solar cells. The second reason is that the diffusion length of the electron is much greater than that of a hole under the same excess carrier density. In general, the diffusion length of an electron is twice or more greater than that of a hole under the same excess carrier density [22]. Moreover, it is known that the depletion region is usually limited to a few micrometers, which is smaller than the main energy deposition region in a fabricated betavoltaic cell [1]. Therefore, the energy deposited outside the depletion region is important for radiation-induced current formation. The design of the p-type region as an emitter layer contributes to improve the charge collection efficiency outside the depletion region in the cell.

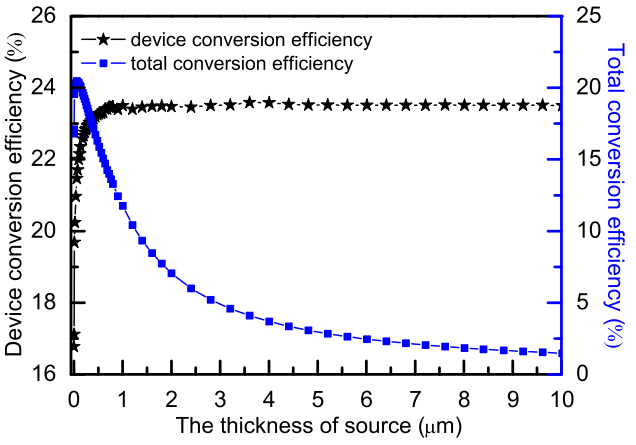

Fig. 13 (Color online) Energy conversion efficiencies versus the thickness of the ^{63}Ni source

For optimal performance of betavoltaic cells, the most important issue is that the depletion region of the energy converter should match the main region of the ionizing radiation well. According to the Shockley equation, for an ideal p–n homojunction, the built-in potential barrier V_{bi} at zero bias voltage is given by [1, 5]

$$V_{\text{bi}} = \frac{k_{\text{B}} \cdot T}{q} \ln \frac{N_{\text{A}} \cdot N_{\text{D}}}{n_{\text{i}}^2}, \tag{9}$$

where N_{A} is the acceptor doping concentration in the p-type region, N_{D} is the donor doping concentration in the p-type region, and n_{i} is the intrinsic carrier concentration. The built-in potential barrier is regarded as the theoretical maximum open-circuit voltage in nuclear battery systems [18]. The width of the depletion region at zero bias voltage is given by [1, 5]

$$W = \left\{ \frac{2\varepsilon_0 \varepsilon_{\text{s}} V_{\text{bi}}}{q} \left(\frac{N_{\text{A}} + N_{\text{D}}}{N_{\text{A}} \cdot N_{\text{D}}} \right) \right\}^{1/2}, \tag{10}$$

where ε_0 is the vacuum dielectric constant and ε_s is the relative dielectric constant (which is 9.7 for 4H–SiC material) [1]. In the 4H–SiC-based junction, when both N_{A} and N_{D} vary between 1×10^{13} and 1×10^{18} cm^3, the built-in potential barrier increases from 2.5 to 3.1 V and the width of the depletion region decreases from 23.2 to 0.08 μm at 300 K. The results are shown in Figs. 14 and 15, respectively. The figures show that the lower doping concentration produces a lower built-in potential barrier and a larger width of the depletion region. In addition, the width of the depletion region is more sensitive than the built-in potential barrier to the doping concentrations. Next, the width of the depletion region, which extends into the p-type region (X_{p}) and the n-doped region (X_{n}) from the metallurgical junction, is given by [22]

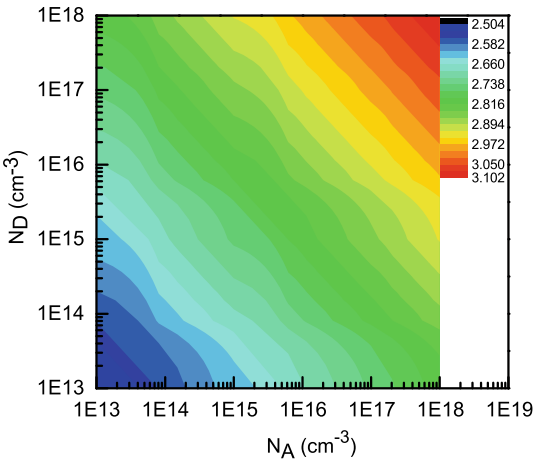

Fig. 14 (Color online) Built-in potential barrier in volts versus the donor and acceptor doping concentration in the 4H–SiC-based junction

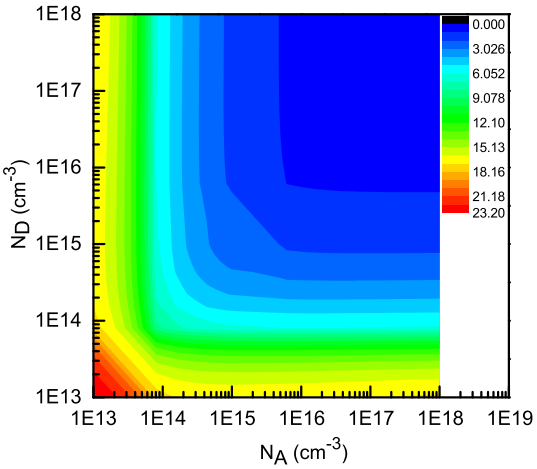

Fig. 15 (Color online) Width of depletion region in μm versus the donor and acceptor doping concentration in the 4H–SiC-based junction

$$X_{\mathrm{p}} = \left\{ \frac{2\varepsilon_0 \varepsilon_{\mathrm{s}} V_{\mathrm{bi}}}{q} \left[\frac{N_{\mathrm{D}}}{N_{\mathrm{A}}} \right] \left[\frac{1}{N_{\mathrm{A}} + N_{\mathrm{D}}} \right] \right\}^{1/2} \tag{11}$$

and

$$X_{\mathrm{n}} = \left\{ \frac{2\varepsilon_0 \varepsilon_{\mathrm{s}} V_{\mathrm{bi}}}{q} \left[\frac{N_{\mathrm{A}}}{N_{\mathrm{D}}} \right] \left[\frac{1}{N_{\mathrm{A}} + N_{\mathrm{D}}} \right] \right\}^{1/2}, \tag{12}$$

respectively. Moreover, the relationship between X_{p} and X_{n} is expressed as $X_{\mathrm{p}}/X_{\mathrm{n}} = N_{\mathrm{D}}/N_{\mathrm{A}}$. Therefore, the design of doping concentrations is the primary method to obtain the appropriate energy converter in betavoltaic cells.

In this research, the depletion region of the energy converter should be $\geq 8\,\mu\mathrm{m}$ and it is better that it extends into the p-type region. From Figs. 14 and 15, we can obtain that when the light doping concentration of the p-type region is $4.7 \times 10^{13}\,\mathrm{cm}^3$, the doping concentration of the n-doped region varies between $5 \times 10^{14}\,\mathrm{cm}^3$ and $1 \times 10^{18}\,\mathrm{cm}^3$, and the width of depletion region is $\sim 8\,\mu\mathrm{m}$. The result is plotted in Fig. 16. The corresponding built-in potential barrier increases from 2.64 to 2.84 V at 300 K, and the values of built-in potential barrier are larger than the theoretical maximum open-circuit voltage in 4H–SiC–^{63}Ni betavoltaic cells. Therefore, the design of doping concentrations mentioned above is reasonable. Furthermore, in Fig. 16, it is shown that, if the light doping concentration of the p-type region is $4.7 \times 10^{13}\,\mathrm{cm}^3$, the doping concentration of the n-type region varies between 3×10^{16} and $1 \times 10^{18}\,\mathrm{cm}^3$, and the depletion region almost extends into the p-type region.

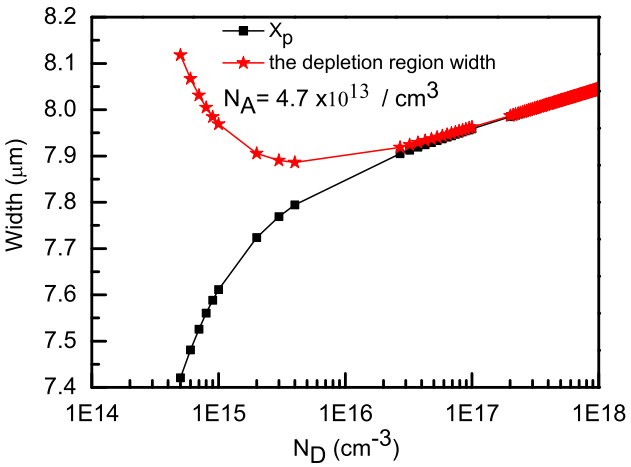

Fig. 16 (Color online) Width of depletion region and the extending width in the p-type region versus the donor doping concentration N_{D} based on the acceptor doping concentration $N_{\mathrm{A}} = 4.7 \times 10^{13}\,\mathrm{cm}^3$ in the 4H–SiC-based junction

Table 2 Theoretical cell parameters

Parameter	Value
J_{sc} (μA/cm^2)	0.152
V_{oc} (V)	2.53
P_{max} (μW/cm^2)	0.36
FF (%)	94.3
η_{dev} (%)	23.5
η_{total} (%)	11.8

Finally, a feasible design of a p–n-junction-based 4H–SiC–^{63}Ni cell is presented. Based on the typical cell structure illustrated in Fig. 6, when the thickness of the ^{63}Ni layer is 2 μm, the thickness of the p-type region is nearly 8 μm, the doping concentration of the p-type region is $4.7 \times 10^{13}\,\mathrm{cm}^3$, and the doping concentration of the n-type region varies between $3 \times 10^{16}\,\mathrm{cm}^3$ and $1 \times 10^{18}\,\mathrm{cm}^3$, the theoretical calculated cell performance nearly reaches its maximum. The results are listed in Table 2. In addition, the whole thickness of the energy

conversion unit should be $> 23\,\mu m$ to prevent beta particles from escaping the device for ^{63}Ni layers with different thicknesses.

5 Conclusion

In summary, 4H–SiC p–n-junction-based betavoltaic batteries with a ^{63}Ni source are investigated. First, the main factors that affect the energy conversion efficiencies of the cells are analyzed. Next, based on the simulation results, theoretical maximum electrical properties and energy conversion efficiencies of the cells are calculated. When the thickness of the ^{63}Ni source increases from 2×10^{-3} to $10\,\mu m$, the theoretical maximum device conversion efficiency increases from 16.77 to 23.51% and the total conversion efficiency decreases from 16.73 to 1.48%. Furthermore, a feasible design with a maximum output power density of $0.36\,\mu W/cm^2$ and an optimal device conversion efficiency of 23.5% is presented. Finally, the results in our work are helpful for realizing an optimal design in the practical fabrication of 4H–SiC–^{63}Ni cells. Moreover, the simulated and calculated model can be used in p–n-junction-based batteries with other semiconductor materials and beta sources.

References

1. M.A. Prelas, C.L. Weaver, M.L. Watermann, A review of nuclear batteries. Prog. Nucl. Energy **75**, 117–148 (2014). https://doi.org/10.1016/j.pnucene.2014.04.007
2. M. Lu, G.G. Zhang, K. Fu, Gallium Nitride Schottky betavoltaic nuclear batteries. Energy Convers. Manag. **52**, 1955–1958 (2011). https://doi.org/10.1016/j.enconman.2010.048
3. X.Y. Li, Y. Ren, X.J. Chen, ^{63} Ni schottky barrier nuclear battery of 4H–SiC. Radioanal. Nucl. Chem. **287**, 173–176 (2011). https://doi.org/10.1007/s10967-010-0746-7
4. X.B. Tang, D. Ding, Y.P. Liu, Optimization design and analysis of Si–^{63} Ni betavoltaic battery. Sci. China. Tech. Sci. **55**, 990–996 (2012). https://doi.org/10.1007/s11431-012-4752-6
5. X.B. Tang, Y.P. Liu, D. Ding et al., Optimization design of GaN betavoltaic microbattery. Sci. China. Tech. Sci. **55**, 659–664 (2012). https://doi.org/10.1007/s11431-011-4739-8
6. F.H. Li, G. Xu, Y.L. Yuan et al., GaN PIN betavoltaic nuclear batteries. Sci. China. Tech. Sci. **57**, 25–28 (2014). https://doi.org/10.1007/s11431-013-5422-z
7. Y.P. Liu, X.B. Tang, Z.H. Xu et al., Optimization and temperature effects on sandwich betavoltaic microbattery. Sci. China. Tech. Sci. **57**, 14–18 (2014). https://doi.org/10.1007/s11431-013-5413-0
8. V. Bormashov, S. Troschiev, A. Volkov, Development of nuclear microbattery prototype based on Schottky barrier diamond diodes. Phys. Stat. Solidi A. **11**, 2539–2547 (2015). https://doi.org/10.1002/pssa.201532214
9. Y.P. Liu, X.B. Tang, Z.H. Xu et al., Influences of planar source thickness on betavoltaics with different semiconductors. Radioanal. Nucl. Chem. **304**, 517–525 (2015). https://doi.org/10.1007/s10967-014-3879-2
10. G. Gui, K. Zhang, J.P. Blanchard, Prediction of 4H–SiC betavoltaic microbattery characteristics based on practical Ni-63 sources. Appl. Radiat. Isot. **107**, 272–277 (2016). https://doi.org/10.1016/j.apradiso.2015.11.001
11. S. Tarelkin, V. Bormashov, E. Korostylev, Comparative study of different metals for Schottky barrier diamond betavoltaic power converter by EBIC technique. Phys. Stat. Solidi A. **9**, 2492–2497 (2016). https://doi.org/10.1002/pssa.201533060
12. F. Rahmani, H. Khosravinia, Optimization of Silicon parameters as a betavoltaic battery: comparison of Si p–n and Ni/Si Schottky barrier. Radiat. Phys. Chem. **125**, 205–212 (2016). https://doi.org/10.1016/j.radphyschem.2016.04.012
13. C. Delfaure, M. Pomorski, J. de Sanoit et al., Single crystal CVD diamond membranes for betavoltaic cells. Appl. Phys. Lett. **108**, 252105:1–252105:4 (2016). https://doi.org/10.1063/1.4954013
14. K. Zhang, G. Gui, P. Pathak et al., Quantitative modeling of betavoltaic microbattery performance. Sens. Actuators A. **240**, 131–137 (2016). https://doi.org/10.1016/j.sna.2016.01.028
15. H. Sadeghi, S.M. Mostajabodavati, A. Eshaghi, Design and simulation of a semispherical semiconductor to construct a betavoltaic battery using *c*-Si and *a*-Si: H materials with different doping concentration. J. Comput. Electron. **15**, 1577–1592 (2016). https://doi.org/10.1007/s10825-016-0896-0
16. C. Thomas, S. Portnoff, M.G. Spencer, High efficiency 4H–SiC betavoltaic power sources using tritium radioisotopes. Appl. Phys. Lett. **108**(013505), 1–4 (2016). https://doi.org/10.1063/1.4939203
17. S. Butera, G. Lioliou, A.B. Krysa, Temperature dependence of an AlInP ^{63} Ni betavoltaic cell. J. Appl. Phys. **120**(144501), 1–5 (2016). https://doi.org/10.1063/1.4964504
18. A.A. Krasnov, V.V. Starkov, S.A. Legotin, Development of betavoltaic cell technology production based on microchannel silicon and its electrical parameters evaluation. Appl. Radiat. Isot. **121**, 71–75 (2017). https://doi.org/10.1016/j.apradiso.2016.12.019
19. H.C. Wu, *Dissertation*. Dalian University of Technology. pp. 20–30 (2005)
20. N.A. Kuruoglu, O. Ozdemir, K. Bozlcurt, Betavoltaic study of a GaN p–i–n structure grown by metal-organic vapour phase epitaxy with a Ni-63 source. Thin Solid Films. **636**, 746–750 (2017). https://doi.org/10.1016/j.tsf.2017.07.033
21. Y.P. Liu, Z.H. Xu, H. Wang, Vacuum degree effects on betavoltaics irradiated by ^{63} Ni with differently apparent activity densities. Sci. China Tech. Sci. **60**, 282–288 (2017). https://doi.org/10.1007/s11431-016-0505-x
22. D.A. Neamen, *Semiconductor Physics and Devices: Basic Principles*, 4th edn. (Publishing House of Electronics Industry, McGraw-Hill Education, Xi'an, 2017), pp. 248–630